

Prediction of structural parameters and physical properties of CsHSO₃ up to 60 GPa

C. Griewatsch and B. Winkler

Mineralogisch-Petrographisches Institut der Christian-Albrechts Universität, Olshausenstrasse 40, D-24098 Kiel, Germany

V. Milman

MSI, 240/250 The Quorum, Barnwell Road, Cambridge CB5 8RE, United Kingdom

C. J. Pickard

Cavendish Laboratory, University of Cambridge, Madingley Road, Cambridge CB3 0HE, United Kingdom

(Received 15 September 1997)

Ab initio calculations based on density-functional theory have been used to predict the position of the hydrogen atom in CsHSO₃ and the pressure dependence of structural parameters and physical properties up to 60 GPa. For the calculations, a generalized gradient approximation, pseudopotentials, and a constant pressure relaxation based on a Broyden-Fletcher-Goldfarb-Shanno algorithm were used. At ambient pressure all calculated structural parameters coincide within 3% with experimental data. The S—H stretch frequency calculated within a frozen-phonon approach matches experimental observations within 2%. The present calculations predict a tetrahedral HSO₃[−] ion with a S—H distance of 1.35 Å. Above 20–30 GPa a framework of HSO₃[−] units, interconnected by trifurcated S—H···O bonds, forms. The pressure dependence of optical properties was also predicted: for 0 (60) GPa the calculations give a double refraction of −0.046 (−0.025) and a dispersion of 0.013 (0.018). [S0163-1829(98)01107-2]

INTRODUCTION

CsHSO₃ crystallizes at ambient conditions in the trigonal space group *R3m* with one formula per unit cell.¹ The experimentally determined structural parameters are given in Table I. It is of course practically impossible to locate the position of a hydrogen in the neighborhood of Cs with x-ray diffraction and as no neutron-diffraction data have been published yet, the position of the H atom had to be inferred by other methods. Johansson *et al.* concluded from a symmetry analysis of IR-spectroscopic data that the hydrogen is bonded to the sulfur atom and a tetrahedral HSO₃[−] group is formed.¹ The existence of such a group has long been controversially discussed because the structure of this unusual group has never been determined directly, but rather has been derived from IR and Raman data.^{1–4} That the HSO₃[−] group can be more stable than another tautomer has recently been demonstrated by Brown and Barber with an *ab initio* study of HSO₃[−] and HOSO₂[−] groups.⁵ Brown and Barber concluded that the former was more stable than the latter both in aqueous solution and as an isolated group.⁵

In CsHSO₃ the proposed HSO₃[−] group occurs in a rather simple structure, which can be investigated with modern *ab initio* calculations based on density-functional theory (DFT). Such calculations can provide detailed atomic models for periodic solids, including a prediction of the position of the hydrogen atom and the pressure dependence of physical properties. The S—H stretch frequencies can easily be calculated by the “frozen-phonon” approach and can serve as a sensitive test of the correct description of the interatomic interaction in the atomic model. The pressure dependence of the structure can also be calculated, thus allowing further insight into the interactions between the HSO₃[−] groups and the Cs cations.

In the following, first we give details of the computations, then we discuss the results for ambient pressure, and finally we present the calculated high-pressure behavior. The paper is concluded by a discussion of the predictions obtained here.

COMPUTER SIMULATION

Commercial (MSI) and academic versions of the software package CASTEP (Cambridge Serial Total Energy Package), which has been described elsewhere by Teter *et al.* and Payne *et al.* and associated programs for symmetry analysis, were used for the calculations presented here.^{6,7} CASTEP is a density-functional-theory–based pseudopotential total-energy code that employs special point integration over the Brillouin zone and a plane-wave basis set for the expansion of the wave functions. The calculations were performed using norm-conserving nonlocal pseudopotentials of the form suggested by Kleinmann and Bylander, where the pseudopotentials were taken from the CASTEP database.⁸ A gradient-corrected form of the exchange-correlation functional [generalized gradient approximation (CGA)] was used in the form suggested by White and Bird.⁹ A cutoff energy of 900 eV (66.2 Ry) was used in all calculations. The Monkhorst-Pack scheme was used to sample the Brillouin zone; ten points were used in the irreducible wedge of the Brillouin zone.¹⁰ Full structural relaxations in the polar space groups *P1* and *R3m* were performed with the cesium atoms fixed at the origin. The Hessian matrix in the mixed space of internal coordinates and the cell variables was updated using *ab initio* calculated atomic forces and the stress tensor. Pulay stress corrections were evaluated numerically by performing total-energy calculations at three different values of the kinetic energy cutoff.¹¹ The calculations were considered converged when forces acting on the atoms were less than 0.05 eV/

TABLE I. Comparison between experimental and calculated structures of CsHSO₃.

Parameter	Experiment ^a	value _{calc} - value _{expt} (%)	Calculated ^b	
			0 GPa	60 GPa
a_0 (Å)	4.6721(7)	+2	4.7799	3.7738
α (deg)	85.31(1)	-3	82.61	89.73
V (Å ³)	101.01(2)	+6	106.70	53.74
x_S	0.4461(3)		0.4489	0.4427
x_O	0.1461(4)		0.1606	0.0925
y_O	0.5293(7)		0.5324	0.5190
x_H			0.5945	0.6384
d S—O (Å)	1.454(2)	-3	1.406	1.381
d S—H (Å)			1.352	1.286
d O—H _{intra} (Å)			2.195	2.161
d O—H _{inter} (Å)			2.666	1.825
\sphericalangle O—S—O (deg)	113.1(2)	± 0	113.1	110.7
\sphericalangle O—S—H (deg)			105.5	108.3
ν_{S-H} (cm ⁻¹)	2579	-2	2518(4)	3098(4)

^aJohansson *et al.* (Ref. 1).^bThis work.

Å and the residual bulk stress was smaller than 0.1 GPa. Calculations were performed for various pressures between 0 and 60 GPa, a pressure range accessible with modern diamond anvil cell methods for both diffraction and spectroscopic experiments. The calculation of optical properties involves several steps. A detailed description can be found in Ref. 12. The wavelength dependence of the refractive index n is calculated by obtaining the matrix transition elements between occupied and unoccupied states. The latter were derived from the Kohn-Sham eigenvalues obtained from the fixed Hamiltonian after reaching self-consistency.

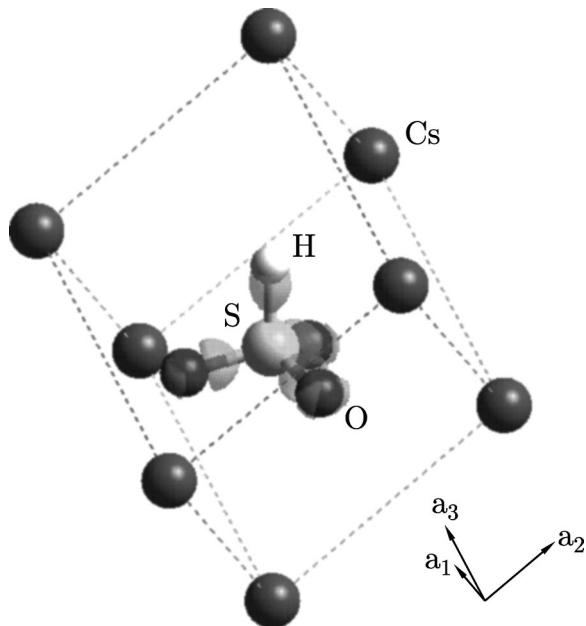


FIG. 1. Computed structure of CsHSO₃ for ambient pressure. In addition, the difference electron density is plotted as a constant value surface showing the covalent S—O and S—H bonds. Furthermore, the one-electron pairs of the oxygen are clearly visible.

STRUCTURE AND PROPERTIES AT AMBIENT PRESSURE

The computed structure at ambient pressure is shown in Fig. 1, whereas the structural parameters are summarized in Table I and Figs. 2 and 3. The calculated data agree with the experimental data within the usual DFT accuracy.

The position of the hydrogen atom can be determined by calculations such as those employed here by starting with a trial structure and calculating the forces acting on the atoms. An unrealistic atomic coordinate will lead to very large forces and geometry optimization will result in a structure very different from the trial one.

After checking that a hydrogen position close to the sulfur atom was indeed a reasonable trial structure, the H atom was fixed by symmetry on the threefold axis. This is necessary as disordered systems currently cannot be investigated without relying on further approximations. Hence the current calculations cannot exclude the possibility of a dynamic disorder

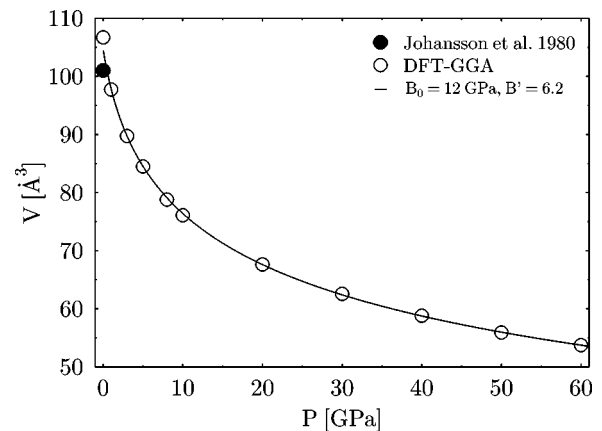


FIG. 2. Pressure dependence of the unit cell volume of CsHSO₃. The black filled circle represents the experimental value obtained by Johansson *et al.* at ambient conditions (Ref. 1). The solid line is a fit with a Birch-Murnaghan equation.

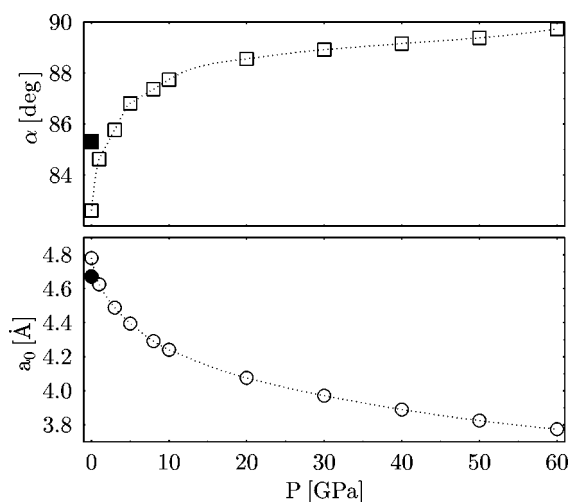


FIG. 3. Pressure dependence of the rhombohedral lattice parameters of CsHSO_3 . The lattice parameter a_0 is plotted with circles and the rhombohedral angle α is plotted with squares. The filled symbols are the experimentally obtained values. The dotted lines are guides to the eye.

of the H atom on an annulus around the threefold axis. A static disorder can be excluded as IR spectroscopy is a “local” probe that does not average over large volumes and long times such as diffraction techniques. There is, however, currently no reason to assume a dynamic disorder and hence the restriction of the search of the hydrogen position to the threefold axis seems reasonable. Furthermore, calculations in the space group $P1$ with the hydrogen atom displaced from the threefold axis towards one of the three neighboring oxygen atoms lead always to unacceptably high forces that prevent a convergence of the calculations. This is remarkable since this atom configuration corresponds to a HOSO_2^- group, which is reasonable from a chemical point of view.

The position of the hydrogen atom obtained from our calculations gives a distance between the sulfur and the hydrogen atom of $d_{\text{S-H}} = 1.35 \text{ \AA}$ and hence our results agree with the tetrahedral form of the HSO_3^- group proposed by Johansson *et al.*¹ An analysis of the valence electron density clearly showed an accumulation of electron density midway between the hydrogen and sulfur, which is consistent with the assumption of a covalent S—H bond (see Fig. 1). The binding forces acting between the sulfur and the hydrogen atom can be probed with quantum-mechanical calculations, and can be compared to the results deduced from vibrational spectroscopy. Here we concentrate on the S—H stretching

frequency. We approximate the eigenvector of the S—H stretching frequency in the solid by assuming that, with the exception of the hydrogen atom, all atomic displacements are zero. This is generally justified as all other atoms are much heavier than hydrogen and it is the mass weighted displacements that are relevant.^{13,14} In other words, we repeated the calculation of the energy with several distinct displacements of the hydrogen along the S—H bond. A plot of the energy against these displacements gave us the potential “felt” by the hydrogen. The potential for ambient pressure is plotted in Fig. 9 together with the potentials calculated for some high-pressure values, which will be discussed below. From the harmonic coefficient of a cubic fit we obtained the force constant of the S—H bond, which allows the calculation of the corresponding frequency. There is only a 2% disagreement between the experimental and the calculated value of the S—H stretching frequency at ambient pressure (Table I), implying that the model calculations correctly reproduce the S—H interaction. The good agreement between the observed and calculated frequency provides further evidence against a HOSO_2^- group in this compound, as the stretching frequency of an OH^- group would be expected to be significantly higher.¹⁵ Only a very strong hydrogen bond could weaken the hypothetical O—H bond sufficiently to shift the O—H stretching frequency by about 1000 cm^{-1} .¹⁵ The topology of the structure makes the formation of such a strong hydrogen bond unlikely.

A comparison of the calculated HSO_3^- geometry with the results obtained by Brown and Barber for an isolated ion is shown in Table II.⁵ The ion in the gaseous phase is computed to have slightly larger bond lengths compared to the HSO_3^- embedded in a crystalline structure, which agrees with the experimentally observed trend. Furthermore, the S—H stretching frequency for the gaseous and aqueous phases calculated by Brown and Barber seems to be lower than the value calculated for the crystalline phase in this work (see Table II).⁵ The experimental data for the aqueous phase [$\nu_{\text{S-H}} = 2543 \text{ cm}^{-1}$ obtained by Herlinger and Long and $\nu_{\text{S-H}} = 2532(3) \text{ cm}^{-1}$ obtained by Simon and Waldmann] and the crystalline phase ($\nu_{\text{S-H}} = 2579 \text{ cm}^{-1}$ obtained by Johansson *et al.*) show the same trend.^{16,17,1} An analysis of the electron density revealed that there was no significant interaction between the hydrogen of one HSO_3^- to the oxygen of another HSO_3^- group at ambient pressure.

STRUCTURE AND PROPERTIES AT HIGH PRESSURES

Pressure-induced changes of structural parameters and physical properties are shown in Figs. 2–11. In order to ana-

TABLE II. Comparison of the HSO_3^- geometry and the S—H stretch frequency calculated by different *ab initio* methods.

Parameter	Hartree-Fock ^a	Density-functional theory ^b	
	aqueous and gaseous phase	crystalline phase	Difference (%)
$d \text{ S—O}$ (\AA)	1.481	1.406	–5
$d \text{ S—H}$ (\AA)	1.371	1.352	–1
$\sphericalangle \text{O—S—H}$ (deg)	103.7	105.5	+2
$\nu_{\text{S-H}}$ (cm^{-1})	2478	2518(4)	+2

^aBrown and Barber (Ref. 5).

^bThis work.

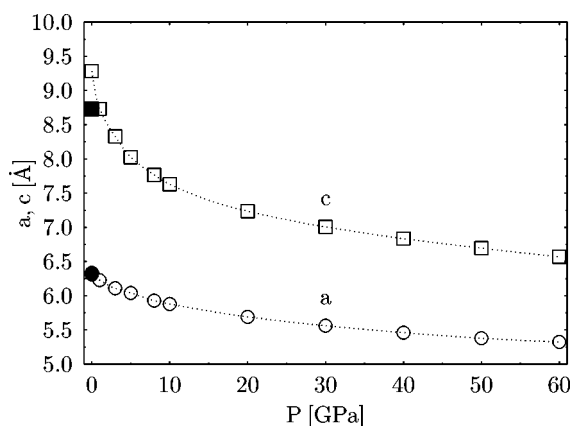


FIG. 4. Pressure dependence of the hexagonal lattice parameters of CsHSO_3 . The lattice parameter a is plotted with circles and c is plotted with squares. The filled symbols are the experimentally obtained values. The dotted lines are guides to the eye.

lyze the pressure dependence of the volume, all data points were fitted with a third-order Birch-Murnaghan equation of state¹⁸

$$p(V) = \frac{3}{2}b \left[\left(\frac{V_0}{V} \right)^{7/3} - \left(\frac{V_0}{V} \right)^{5/3} \right] \times \left\{ 1 + \frac{3}{4}(b' - 4) \left[\left(\frac{V_0}{V} \right)^{2/3} - 1 \right] \right\}, \quad (1)$$

where V_0 is the unit-cell volume at zero pressure, b denotes the bulk modulus, and $b' = \partial b / \partial p$ at $p=0$. The values obtained from the fit are $V_0 = 105(1) \text{ \AA}^3$, $b = 12(1) \text{ GPa}$, and $b' = 6.2(2)$. V_0 is in good agreement with the calculated value for 0 GPa. The values for b and b' show that CsHSO_3 is twice as soft as NaCl ($b_{\text{NaCl}} = 24.19 \text{ GPa}$).¹⁹

With increasing pressure the lattice parameter a_0 decreases, whereas the rhombohedral angle α increases (Fig. 3). The value of α varies approximately linearly with pressure above approximately 20 GPa. The hexagonal description of the structure gives a better insight into the mechanism of the compression. In Fig. 4 the pressure dependence of the hexagonal axes are plotted. The value of the lattice parameter a at ambient pressure shows a much better agreement with the experimental value than the lattice parameter c that is parallel to the S—H bond. Whether this is an artifact or an inaccuracy caused by the interactions involving hydrogen is not clear. But the good agreement of the S—H stretching frequency indicates the accuracy in modeling the S—H bond. In Fig. 5 the much stronger compression of the c axis compared to the a axis can be seen. This is due to the weaker interactions via the hydrogen atom.

Under compression, CsHSO_3 shows the typical behavior of a molecular crystal. This is evident from Figs. 6–8, which show that the intramolecular S—O, S—H, and O—H distances are nearly constant within the investigated pressure range, while the “intermolecular” CS—O, O—H, and S—H \cdots O distances show a strong pressure dependence. The size of the HSO_3^- tetrahedron is therefore nearly pressure independent, reflecting the difference of the stiffness of the covalent intramolecular bonds from the much weaker intermolecular interactions. An application of pressure in ex-

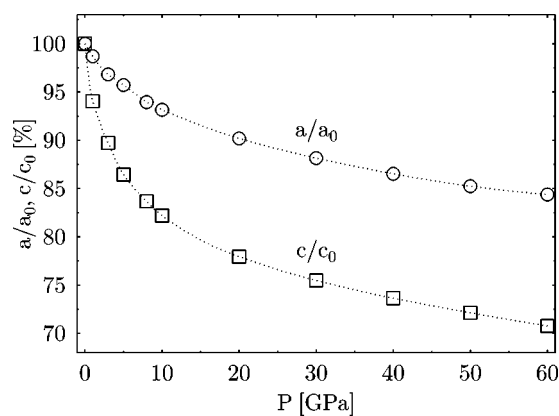


FIG. 5. Pressure dependence of the relative length of the hexagonal lattice parameters of CsHSO_3 . The lattice parameter a is plotted with circles and c is plotted with squares. The dotted lines are guides to the eye.

cess of approximately 20 GPa leads to a S—H \cdots O distance shorter than 2.8 \AA and an intermolecular O—H distance shorter than 2.0 \AA . Thus, considering the van der Waals radii, there is evidence for an existing “hydrogen-bond interaction” above 20 GPa.²⁰ In CsHSO_3 it is not clear if the use of the term “hydrogen bond” is justified. Generally, a hydrogen bond is of the form $R^{\delta-} - \text{H} \cdots R'^{\delta-}$, but in CsHSO_3 the sulfur atom is positively charged. Although the intermolecular interaction between the hydrogen and the oxygen atom is most likely to be attractive, we will show below that the behavior of the S—H stretching frequency does not agree with the behavior of the R—H stretching frequency in a conventional hydrogen bond. In the absence of a better term, we will therefore designate the supposedly weakly binding interaction between the hydrogen of one HSO_3^- group with an oxygen atom of another group as the S—H \cdots O interaction. There is no significant discontinuity in the pressure dependence of any of the structural parameters or physical properties and hence the strength of the S—H \cdots O interaction seems to change continuously. An analysis of the valence electron density also gives clear in-

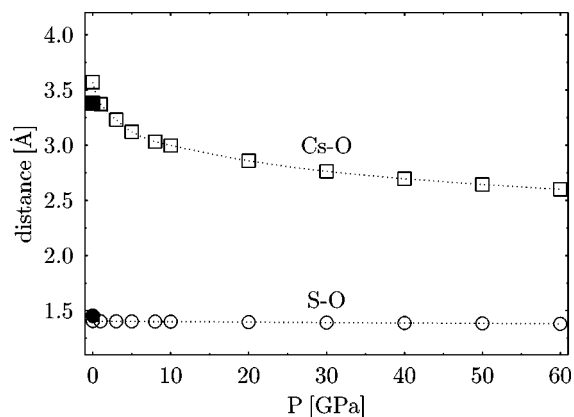


FIG. 6. Pressure dependence of interatomic distances. The intramolecular S—O distance, plotted with circles, is nearly pressure independent, whereas the intermolecular Cs—O distance, plotted with squares, shows a strong pressure dependence. The filled symbols are the experimentally obtained values. The dotted lines are guides to the eye.

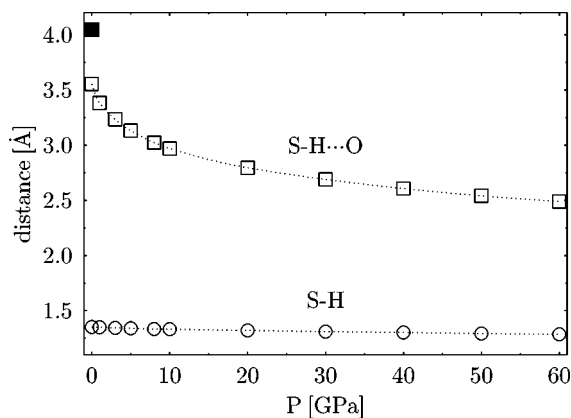


FIG. 7. Pressure dependence of interatomic distances. The intramolecular S—H distance, plotted with circles, is nearly pressure independent, whereas the intermolecular S—O distance, plotted with squares, shows a strong pressure dependence. The filled symbols are the experimentally obtained values. The dotted lines are guides to the eye.

indications of a weak interaction between the HSO_3^- ions at approximately above 20 GPa. Hence, while at ambient pressure CsHSO_3 has a structure dominated by ionic bonding between the Cs cations and the HSO_3^- anions, above approximately 20 GPa the HSO_3^- ions build a framework interconnected by trifurcated S—H \cdots O bonds, whose strength is assumed to increase with increasing pressure. The cesium atoms then lie in the cages of this framework, where each of them is surrounded by eight HSO_3^- ions.

In addition to the geometry optimization we computed the pressure dependence of the S—H stretch frequency similar to the calculations at ambient pressure described above (Fig. 9). The pressure dependence of these frequencies is plotted in Fig. 10. The pressure-induced frequency shift is not linear over the pressure range investigated. Rather, there seems to be a change in the slope at about 15 GPa, which becomes more obvious when the frequency shift is analyzed in terms of the mode Grüneisen parameter $\gamma = -\partial \ln \nu_{\text{S-H}} / \partial \ln V$ (see Fig. 10).²¹

This behavior is different from the pressure-induced shift of O—H stretching frequencies due to increasing hydrogen

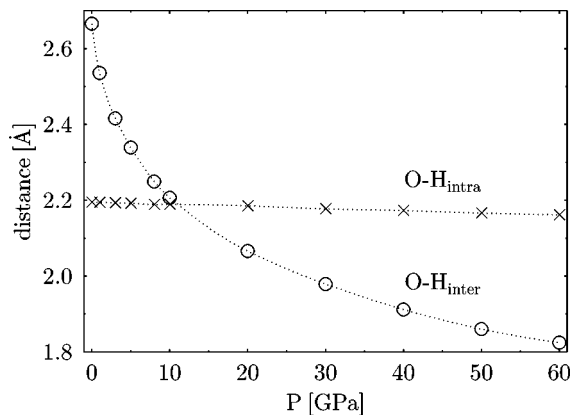


FIG. 8. Pressure dependence of the interatomic O—H distances. The intramolecular O—H distance, plotted with crosses, is nearly constant within the studied pressure range, while the intermolecular O—H distance, plotted with circles, decreases greatly with increasing pressure.

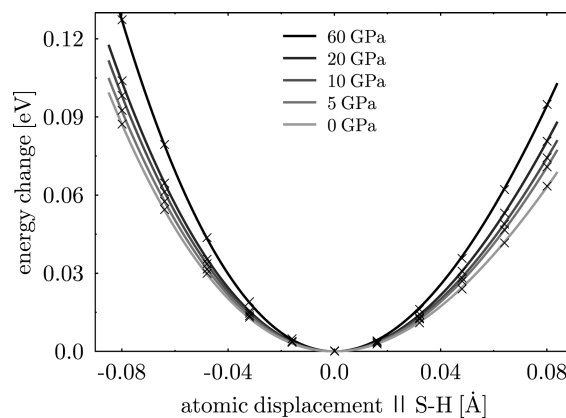


FIG. 9. The “frozen-phonon” approach leads to a potential that is related to the S—H bond. From the curvatures of the potentials the frequencies of the S—H stretching motion (Fig. 10) can be obtained for the respective pressures. The lines are cubic fits to the data.

bonding. Winkler *et al.* observed a decrease of about $0.34 \text{ cm}^{-1} \text{ GPa}^{-1}$ in zoisite, which can be explained in terms of the weakening of the O—H bond due to an increasing strength of the O—H \cdots O bond.²² If the S—H \cdots O bond were similar to a conventional hydrogen bond, the same behavior would have been expected. Instead, we observe that with increasing pressure both the S—H bond and the S—H \cdots O distance decreases, even though the former effect is relatively small compared to the latter. This results in a decrease of the intermolecular O—H distance. This looks like an interaction that “pushes” the hydrogen atom towards the sulfur strengthening the S—H bond and thus increasing the S—H stretching frequency with increasing pressure. Nevertheless, it is possible that above 60 GPa when the O—H distance is even shorter the behavior will change and the S—H bond will start to increase again as in common hydrogen bonds.

In Fig. 11 we present the pressure dependence of some optical properties of solid CsHSO_3 . According to the sym-

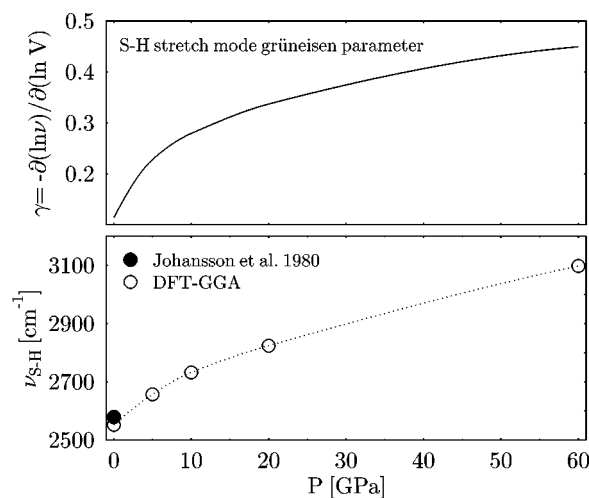


FIG. 10. The pressure dependence of the S—H stretch frequency calculated with a frozen-phonon approach is plotted with open circles whereas the Grüneisen parameter γ is plotted with a solid line. The filled circle shows the experimental value for the frequency. The dotted line is a guide to the eye.

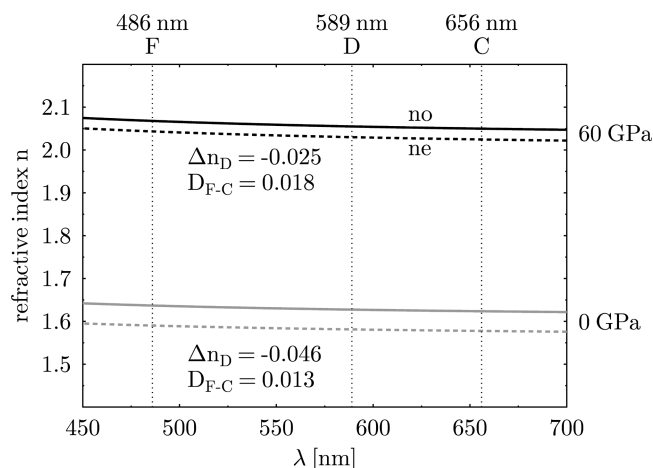


FIG. 11. Predicted pressure dependence of optical properties of CsHSO_3 . While the double refraction ($\Delta n_D = n_e - n_o$ at $\lambda = 589$ nm) is halved from 0 to 60 GPa, the dispersion ($D_{F-C} = \bar{n}_F - \bar{n}_D$) slightly increases. The solid (dashed) line shows the calculated dispersion curve for the ordinary (extraordinary) beam.

metry, the crystal is uniaxial. The calculated optical character is negative with a double refraction $\Delta n_D = n_e - n_o$ of -0.046 at 0 GPa and -0.025 at 60 GPa, respectively. Furthermore, the mean refractive index increases clearly with increasing pressure. There is an intrinsic uncertainty in determining the absolute value of the refractive index, which is related to the underestimation of the band gap in DFT calculations. Hence the refractive indices will most probably be systematically shifted with respect to experiment. In contrast to this, the differences between the optical density at ambient and high

pressure and between the n_e and n_o curves should have a much higher accuracy. Further experimental study is needed to verify this prediction.

SUMMARY AND DISCUSSION

At ambient pressure the calculations presented here predict a tetrahedral HSO_3^- ion in the crystalline modification of CsHSO_3 . The calculated S—H stretch frequency is in good agreement with the experimental data and thus the binding forces between the sulfur and hydrogen atom are modeled correctly. This is a strong argument for the existence of the HSO_3^- group and excludes the alternative explanation based on a HOSO_2^- group. The pressure dependence of the structural parameters is typical for molecular crystals. The volume decrease is due to the decrease of the intermolecular HSO_3^- distances while the size of the HSO_3^- tetrahedra remains nearly constant. From a crystal chemical point of view, the high-pressure behavior is of interest, as the formation of three equal intermolecular S—H \cdots O distances at pressures above 20–30 GPa leads to intermolecular interactions, which, from an electrostatic point of view, should be attractive, but which seem not to be strong enough to weaken the S—H bond. High-pressure powder neutron diffraction and single crystal growth experiments are currently under way to elucidate the reliability of the predictions presented here.

ACKNOWLEDGMENT

The authors would like to thank the Deutsche Forschungsgemeinschaft for financial support (Grant Nos. Wi1232/1-3 and De 412/13-1).

- ¹L.-G. Johansson, O. Lindqvist, and N.-G. Vannerberg, *Acta Crystallogr. B* **36**, 2523 (1980).
- ²A. Simon and W. Schmidt, *Z. Elektrochem.* **64**, 737 (1960).
- ³I. C. Hisatsune and J. Heicklen, *Can. J. Chem.* **53**, 2646 (1975).
- ⁴B. Meyer, L. Peter, and C. Shaskey-Rosenlund, *Spectrochim. Acta A* **35**, 345 (1979).
- ⁵R. E. Brown and F. Barber, *J. Phys. Chem.* **99**, 8071 (1995).
- ⁶M. P. Teter, M. C. Payne, and D. C. Allan, *Phys. Rev. B* **40**, 12 255 (1989).
- ⁷M. C. Payne, M. P. Teter, D. C. Allan, T. A. Avias, and J. D. Joannopoulos, *Rev. Mod. Phys.* **64**, 1045 (1992).
- ⁸L. Kleinmann and D. M. Bylander, *Phys. Rev. Lett.* **48**, 1425 (1982).
- ⁹J. A. White and D. M. Bird, *Phys. Rev. B* **50**, 4954 (1994).
- ¹⁰H. J. Monkhorst and J. D. Pack, *Phys. Rev. B* **13**, 5188 (1976).
- ¹¹G. P. Francis and M. C. Payne, *J. Phys.: Condens. Matter* **2**, 4395 (1990).
- ¹²C. J. Pickard, M. C. Payne, L. M. Brown, and M. N. Gibbs, *Inst. Phys. Conf. Ser.* **147**, 211 (1995).
- ¹³B. Winkler, V. Milman, B. Hennion, M. C. Payne, M.-H. Lee, and J. S. Lin, *Phys. Chem. Miner.* **22**, 461 (1995).
- ¹⁴M. Chall, B. Winkler, and V. Milman, *J. Phys.: Condens. Matter* **8**, 9049 (1996).
- ¹⁵A. Novak, *Struct. Bonding (Berlin)* **18**, 177 (1974).
- ¹⁶A. W. Herlinger and T. V. Long II, *Inorg. Chem.* **8**, 2661 (1969).
- ¹⁷A. Simon and K. Waldmann, *Z. Anorg. Allg. Chem.* **231**, 135 (1955).
- ¹⁸F. Birch, *J. Geophys. Res.* **83**, 1257 (1978).
- ¹⁹R. F. S. Hearmon, in *The Elastic Constants of Crystals and Other Anisotropic Materials*, edited by K. H. Hellwege and A. M. Hellwege, Landolt-Börnstein, New Series, Group III, Vol. 11, Pt. 1 (Springer-Verlag, Berlin, 1979).
- ²⁰J. C. Speakman, *The Hydrogen Bond and Other Intermolecular Forces*, Vol. 27 of *Monographs for Teachers* (The Chemical Society, London, 1975).
- ²¹J.-P. Poirier, in *Introduction to the Physics of the Earth's Interior*, Vol. 3 of *Cambridge Topics in Mineral Physics and Chemistry*, edited by A. Putnis and R. C. Liebermann (Cambridge University Press, Cambridge, 1991).
- ²²B. Winkler, K. Langer, and P. G. Johannsen, *Phys. Chem. Miner.* **16**, 668 (1989).